Enzymatically synthesized dextran nanoparticles and their use as carriers for nutraceuticals

ARTICLE · JULY 2014

DOI: 10.1039/C4FO00103F

4 AUTHORS:

David Semyonov

5 PUBLICATIONS **61** CITATIONS

SEE PROFILE

Ory Ramon

Technion - Israel Institute of Technology

41 PUBLICATIONS **761** CITATIONS

SEE PROFILE

Yuval Shoham

Technion - Israel Institute of Technology

175 PUBLICATIONS **6,672** CITATIONS

SEE PROFILE

Eyal Shimoni

Strauss Group Inc.

72 PUBLICATIONS **1,992** CITATIONS

SEE PROFILE

Food & Function

PAPER

View Article Online
View Journal

Cite this: DOI: 10.1039/c4fo00103f

Enzymatically synthesized dextran nanoparticles and their use as carriers for nutraceuticals

David Semyonov,* Ory Ramon, Yuval Shoham and Eyal Shimoni

Received 12th February 2014
Accepted 13th July 2014

DOI: 10.1039/c4fo00103f

www.rsc.org/foodfunction

This study evaluated the use of enzymatically synthesized dextran nanoparticles to entrap a hydrophobic nutraceutical, the isoflavone genistein. The focus was on the synthesis of pure dextran as the material for the entire nanoparticle, and their inclusion-complexation of genistein. Under optimal conditions (pH 5.2–6 and sucrose concentration >0.5 M), dextransucrase generated spherical dextran nanoparticles (100–450 nm). The two nutraceutical inclusion methods were DMSO dilution in water and acidification. Optimization of the inclusion processes produced nanosized dextran particles containing genistein. The DMSO method was found to be more suitable for inclusion of genistein in dextran, resulting in a higher genistein load (5.6 ± 0.1 g genistein per 100 g particles), and a higher percentage of nanosized particles (85%, 105–400 nm). For both protocols, addition of a freeze-drying step exerted a positive effect presumably due to the formation of new hydrogen bonds and van der Waals interactions.

Introduction

All foods are functional to some extent, because they provide taste, aroma and nutritional value. However nowadays, foods are also being intensively examined for added physiological benefits, such as reduced risk of chronic diseases or otherwise optimized health. Thus, there is a growing global interest in "functional foods". Many attempts at developing functional foods that carry added value (beyond their nutritional value) have been made. Such attempts include enrichment and fortification of foods with bioactive ingredients, such as polyphenols, carotenoids, fatty acids and their derivatives, amino acids, peptides, proteins, vitamins, minerals, and even live probiotic bacteria.[1] Nevertheless, the addition of nutraceuticals and micronutrients presents a major scientific and technological challenge. Many of these bioactive ingredients are chemically and physically labile under food-processing conditions as well as under digestive reactions. In addition, many nutraceuticals are not soluble in water and as a result, are not absorbed in the gut into the bloodstream, limiting their accessibility and availability. Consequently, several studies have looked into the development of food-grade delivery systems that can protect nutraceutical bioactivity through processing and storage with improved water solubility, thermal stability, bioavailability, sensory attributes and physiological performance while controlling and targeting their release.[2–6]

Nutraceuticals such as flavonoids are among the most abundant antioxidants in our diet. Their health effects have come to the attention of nutritionists due to their anti-inflammatory and antioxidative properties, as well as their effect on metabolic syndrome *via* interaction with various nuclear receptors.[7] Chemically, flavonoids are polyphenolic compounds comprised of a 15-carbon (C) backbone with two aromatic rings connected by a 3-C bridge. Flavonoids exist naturally as aglycones, glycosides, or their methylated derivatives. Whereas both sugars and hydroxyl groups increase the water solubility of flavonoids, other substituents, such as methyl groups, make them more lipophilic.[8]

The isoflavone genistein (Fig. 1) is one of the aglycone forms of the isoflavone family; it shows estrogen-like effects and is therefore also known as phytoestrogen,[9] and is found almost exclusively in leguminous plants, with the highest concentration occurring in soybeans.[8] Genistein (4′,5,7-trihydroxyisoflavone) has been identified as the predominant isoflavone in soybean-enriched foods in Asian countries,[10] and is thought to be responsible for many beneficial health effects.[10–14] However, the use of genistein in foods and beverages is restricted due to its poor solubility in water.[15] This characteristic also significantly reduces its bioavailability.[15,16]

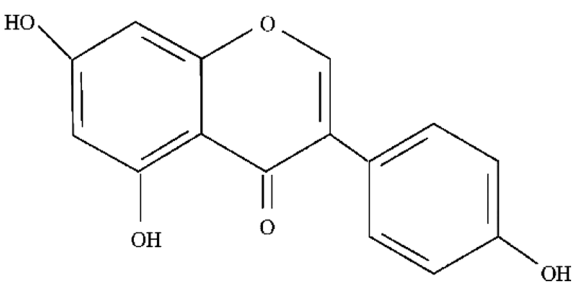

Fig. 1 Molecular structure of the aglycone genistein.

Faculty of Biotechnology and Food Engineering, Technion – Israel Institute of Technology, Haifa 32000, Israel. E-mail: davids@technion.ac.il; Fax: +972-4-8293399; Tel: +972-4-8295645

Fundamental thermodynamic and mass-transfer considerations have revealed that, nanoparticles of no more than 100 nm in diameter should be applied in order to generate a broad-spectrum delivery system. However, experimental data reveal that, in some cases, even nanoparticles in the 100–1000 nm range are capable of producing substantial improvement in the bioavailability of active ingredients.[17] In most cases, this improvement in bioavailability seems to be linked to direct uptake of the nanoparticle. In addition, the direct nanoparticle uptake is controlled by the size and surface chemistry of the nanoparticle system. Nanoparticles in foods provide advantages such as: increased surface area, enhanced solubility, increased rate of dissolution, increased oral bioavailability, lower dosages, protection of drug from degradation, more rapid onset of therapeutic action, and better achievement of drug targeting.[18] Owing to the greater surface area of nanoparticles per volume and/or mass unit, the dissolution rate will be enhanced, increasing the drug's bioavailability relative to that of a drug entrapped in larger-sized particles of the same chemical composition. This offers several prospects for food applications as well, such as increasing the bioavailability of poorly soluble nutraceuticals in functional foods.[19]

In previous studies, solubility and dissolution rate of the isoflavone genistein were found to have increased nine-fold when genistein was incorporated into polymeric nanoparticles such as Eudragit 100 (ref. 20) or polyethylene glycol (PEG) microparticles.[21] Other studies revealed that amylose based complexes can serve as vehicles for delivery, protecting polyunsaturated fatty acids and flavonoids (isoflavones) from oxidation, thermal abuse and the acidic environment of the stomach,[22,23] while nanocomplexes of genistein with β-cyclodextrin[24] were much more water-soluble than genistein alone. Polysaccharides are an appropriate choice as carriers for the delivery of nutraceuticals, based on controlled-release mechanisms such as: time, pH and/or pressure, and sensitivity to bacterial fermentation in the colon or degradation by pancreatic enzymes.[25]

The present study explored whether enzymatic synthesis provides significant advantages over the use of standard polysaccharides as carriers for nutraceuticals. Our hypothesis was that controlled enzymatic synthesis would produce polysaccharides and oligosaccharides with controlled structures, and thus different properties, the size of which could be tailored in the 100–400 nm range. Thus, the main objective of the present study was to develop nanosized molecular vehicles of polysaccharide derivatives, produced from dextran by enzymatic synthesis, which could contain a water-insoluble nutraceutical, the isoflavone genistein. The originality of this work lies in the use of pure enzymatically synthesized dextran as the material for the entire nanoparticle instead of only its coating or making a copolymer. It is now recognized that many metallic nanoparticles are not suitable biomaterials and therefore, making the entire nanoparticle out of this polysaccharide is an advantage. These vehicles would be used to incorporate and stabilize the guest molecule, creating a smart structural design for genistein-delivery systems as a platform for delivering additional nonsoluble bioactive chemicals in foods and/or pharmaceuticals. We expect that our study will generate new solutions to the problem of stabilizing hydrophobic bioactive compounds in foods and drugs, increasing their bioavailability and incorporating them into an enzymatically tailored biopolymer nanoparticle with controlled physical and structural properties.

Results and discussion

The purpose of this study was twofold: (1) to develop an enzymatic procedure for producing dextran nanoparticles as appropriate vehicles for nutraceutical delivery; (2) to include a nutraceutical—the isoflavone genistein—in these nanoparticles for improving flavonoid bioavailability through its nanoencapsulation and particle-size reduction.

We have investigated an enzymatic approach to produce a variety of dextran-based nanoparticles with diverse structures and interesting capabilities. Dextransucrase polymerization of glucose units was explored under various conditions with the aim of synthesizing dextran nanoparticles that could include and complexate bioactive molecules such as genistein. Different reactions with dextransucrase were carried out in the presence of the sucrose substrate.

Effect of pH on the synthesis of dextran nanoparticles

The enzymatic reaction was carried out using a commercial preparation of dextransucrase from *Leuconostoc mesenteroides* D9909. All known dextransucrases belong to Glycoside hydrolase family 70 (GH70) which operate *via* a retaining mechanism and utilize two catalytic acidic residues. To follow the enzymatic reaction the increase in turbidity was recorded over time. The effect of pH was studied by performing the reaction at various pH conditions. Sucrose conversion by dextransucrase yields glucose, which can be incorporated into the growing polymer (formation of dextran) and fructose in a 1 : 1 ratio to the amount of sucrose converted.[26] The amount of sucrose utilized during the reaction (total activity)

Table 1 Effect of pH on final turbidity and substrate (50 mM sucrose) utilization by dextransucrase (0.42 U mL^{-1})

pH	Total sucrose utilization (%)	Glucose assimilated to dextran polymer (%)	Final turbidity (OD_{600})
5.2	100	96	0.62
6	95	93	0.67
7	7	53	0.09
8	0.7	69	0.28

was 100–95% at the lower pH (5.2–6), and only 7–0.7% at higher pH (7–8) (Table 1). In addition, the polymerization activity (percentage of the glucose assimilated to dextran polymer) was 96–93% at the lower pH (5.2–6), and 53–69% at higher pH (7–8). The highest rate in turbidity increase and the highest final turbidity were achieved at pH 5.2 (Fig. 2A). At higher pH no turbidity was obtained due to the sedimentation of what appears to be large dextran aggregates. These aggregates could be resuspended but then quickly settled in the tube (Table 1). DLS measurements of the synthesized dextran (Fig. 2B) revealed that at pH 5.2–6, the particles were 200–400 nm, whereas at higher pH, larger dextran particles, up to 3000 nm, were produced.

Similar results were obtained by Kim *et al.*,[27] who investigated the dextransucrase activity at pH values of 4.5–6.0; they have shown that increasing pH significantly increased the percentage of very-high-molecular-weight dextran particles ($\geq 10^6$). This trend was found to continue in this study at higher pH values (6.7–8.0). We therefore concluded that pH 5.2 is optimal for obtaining relatively small dextran particles that could be useful as carriers for nutraceuticals.

Effect of sucrose concentration on the enzymatic synthesis of dextran

Increasing sucrose concentration in the reaction led to a decrease in the yield of synthesized dextran (Fig. 3A). At low concentrations of sucrose (up to 0.5 M), synthesis resulted in a high yield of dextran (~100%). At 1 M sucrose, dextran yield was approximately 50%. At more than 2 M sucrose, dextran yield tended toward zero. As shown in Fig. 3B, the particles sizes of the reaction products are in the nanometer range (150–500 nm). Two trends can be observed and these trends are correlated with the percent yield of synthesized dextran. First, at low sucrose concentrations (2–200 mM), the synthesized dextran nanoparticles' average size and distribution increase with increasing sucrose concentration. However, at the high concentrations (1–3 M) at which sucrose inhibits dextran synthesis, the dextran yield percent starts to decline, and a decrease in the synthesized dextran's average size and size distribution occurs. These results can be explained by substrate inhibition which is known to occur with these types of enzymes. The exact inhibition mechanism is difficult to reveal since there are several possible products in the reaction.[26,28–32]

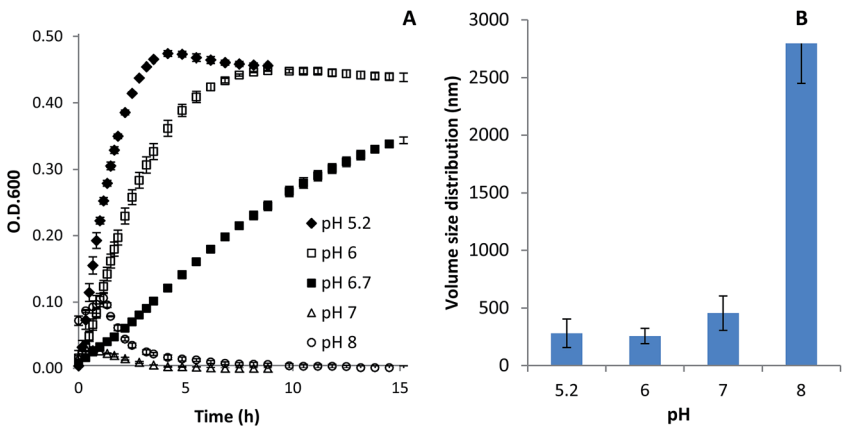

Fig. 2 Effect of pH (5.2–8) during dextran synthesis (0.42 U mL^{-1} dextransucrase and 50 mM sucrose) on (A) turbidity and (B) volume size distribution of the synthesized products measured by DLS.

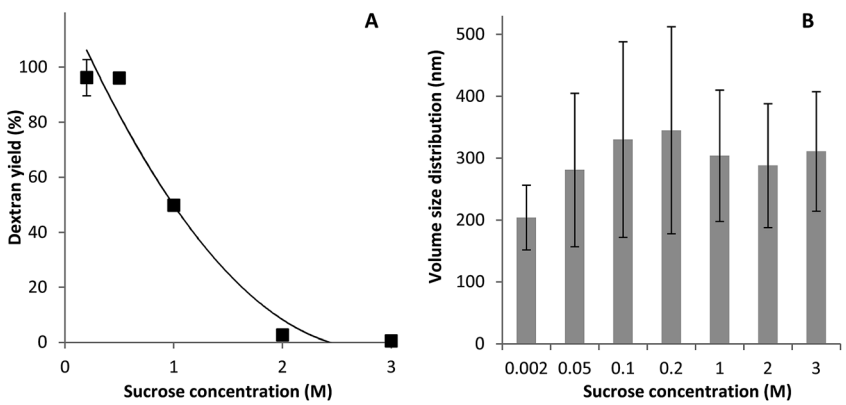

Fig. 3 Effect of sucrose concentration on (A) synthesized dextran yield ($R^2 = 0.986$), and (B) volume size distribution determined by DLS.

Morphology and structure of the nanoparticles generated by dextransucrase

The detailed morphology of the reaction products was determined by cryo-TEM. The relatively rapid freezing rate in liquid nitrogen results in an intact frozen sample, preventing structural changes produced by dehydration. The effects of dextransucrase and substrate concentrations on the particle morphology were investigated. Cryo-TEM images of the dextransucrase reaction products (Fig. 4) displayed well-defined spheroidal particles, the size and density of which were affected by the enzyme-to-substrate ratio. Synthesis at a low dextransucrase concentration (0.2 U mL^{-1}) and high sucrose concentration (21 mM) resulted in spheroidal particles with diameters in the range of 200–300 nm (the DLS measurements showed a volume size distribution of 260 ± 100 nm). Synthesis at the higher dextransucrase concentration of 0.42 U mL^{-1} and a lower sucrose concentration (2 mM) resulted in denser (darker) particles with diameters in the range of 100–180 nm (DLS volume size distribution: 26% 98 nm and 74% 216 nm). Thus, the nanoparticles' dimensions can be controlled by changing enzyme and substrate concentrations. Because of the spherical self-assembly of dextran in water, we assumed that the inner part of these nanoparticles is more hydrophobic than their surface. Therefore, one can speculate that these spherical dextran nanoparticles can serve as nanovehicles for hydrophobic molecules and complexes, because hydrophobic interactions and hydrogen bonding should prevail.

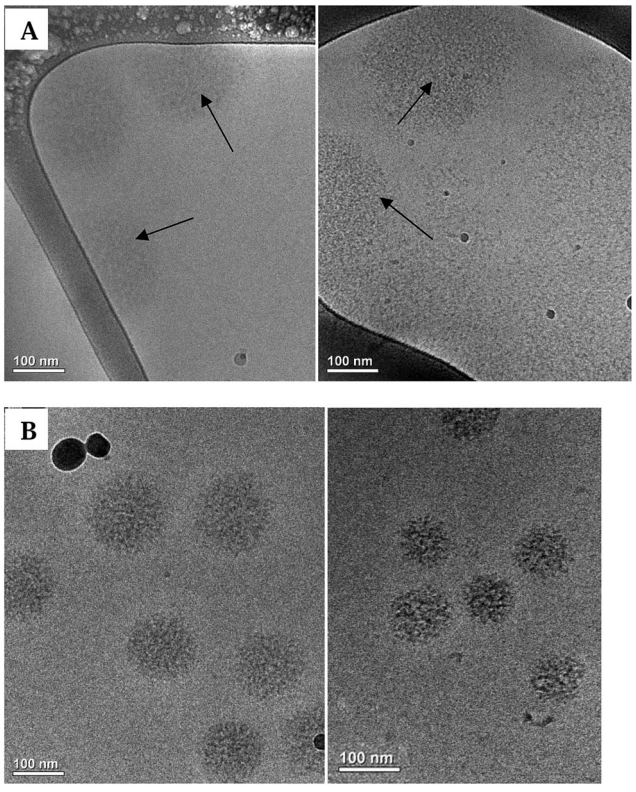

Fig. 4 Cryo-TEM images of the enzymatically synthesized product. (A) Dextransucrase (0.2 U mL^{-1}) and sucrose (21 mM) diluted 10^{-1}-fold, and (B) dextransucrase (0.42 U mL^{-1}) and sucrose (2 mM).

Enzymatically synthesized dextran nanoparticles as vehicles for genistein

Poorly soluble nutraceuticals have been shown to be unpredictably and slowly absorbed relative to those with higher solubility. Their oral bioavailability is controlled by their dissolution rate and can be increased by decreasing the degree of crystallinity and particle size. Several methods have been used to improve the solubility of poorly water-soluble ingredients,[33,34] such as the isoflavone genistein, by entrapping them into nano- and micro-particles, leading to significant improvement of their solubility and performance.[21,22,35] However, to achieve successful implementation of such methodologies, it is essential to understand and control the characteristics of enzymatically synthesized dextran nanoparticles containing genistein. We have evaluated the effect of processing parameters on the yield percentage and encapsulation efficiency, as well as the influence of the nanoparticles' physicochemical characteristics on genistein's dissolution rate and thus on its bioavailability.

Properties of synthesized dextran nanoparticles containing genistein. To determine whether a hydrophobic moiety such as genistein can be included and complexes can be created with the enzymatically synthesized spherical dextran nanoparticles, we have evaluated two protocols: (1) creation of complexes *via* dilution of DMSO in water, and (2) complexation by lowering the aqueous solution pH. Dextran showed solubility in both solutions after a few hours at 90 °C. The dissolution of dextran in DMSO or in alkaline solution is characterized by opening of its globular particle. Dextran particles that were dissolved and then "closed" *via* acidification were nanosized (150–350 nm) (Fig. 5), similar to the particle sizes before the "opening and closing" process. Similar behavior was observed with dextran particles that were dissolved in DMSO and then "closed" in water, displaying a nanometric structure (180–400 nm) with a particle size similar to that before the "opening and closing" process. Morphological characterization by cryo-TEM (Fig. 6A)

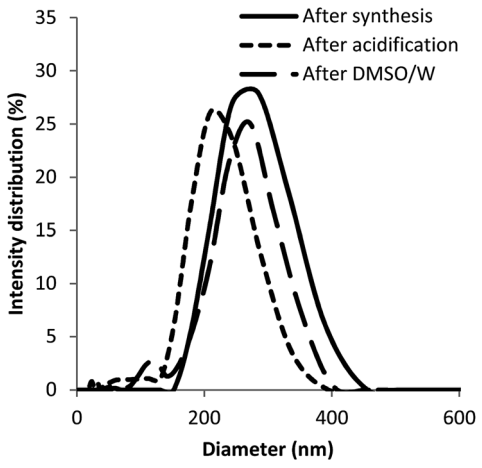

Fig. 5 Size distribution of dextran particles measured by DLS after synthesis (0.1 U mL^{-1} dextransucrase, 150 mM sucrose), and after precipitation by the acidification or DMSO–water (DMSO–W) method.

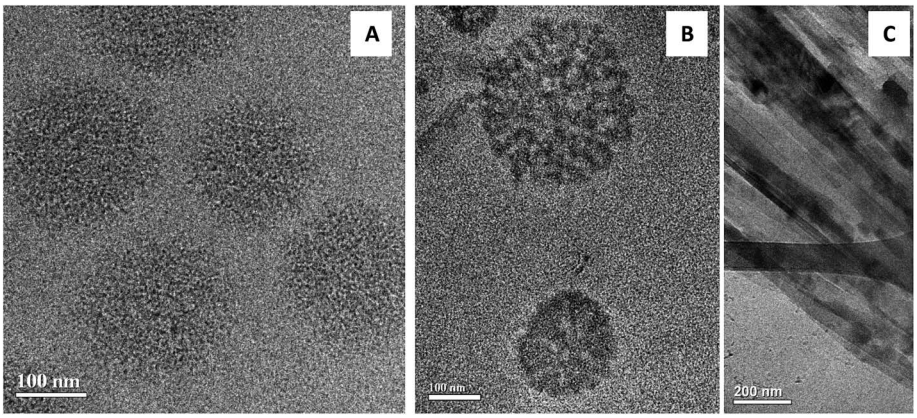

Fig. 6 Cryo-TEM images of dextran–genistein inclusion products. Freeze-dried dextran and genistein were solubilized in DMSO followed by dilution with water, leading to precipitation of the polysaccharide–guest complexes. (A) Dextran without genistein, (B) dextran–genistein at a ratio of 20 : 1 w/w, and (C) genistein.

Table 2 Particle volume size distribution of the dextran–genistein coprecipitation products

Inclusion method		Particle diameter distribution (nm)	A/V_p (m^2 mL^{-1})	A/V_p (m^2 mL^{-1}) of the genistein-loaded dextran
Acidification	Dextran–genistein[a]	125–225 (13%) 740–1000 (16%) >2500 (71%)	2.6 ± 0.03	40.3 ± 10.7
	Genistein[b]	130–175 (0.3%) 1100–2200 (35.5%) >3000 (64.2%)	2.4 ± 0.2	—
DMSO–water	Dextran–genistein[a]	105–400 (85%) >3000 (15%)	10.3 ± 2.2	26.2 ± 10.5
	Genistein[b]	150–270 (0.6%) >3000 (99.4%)	2.0 ± 0.0	—

[a] $n = 6$. [b] $n = 2$.

showed that the dextran particles regain the globular structure exhibited before the dissolution and precipitation.

Following the characterization and control of the dextran "opening and closing" process by both acidification and DMSO–water methods, we have determined whether the enzymatically synthesized dextran can form a "closed" core that will entrap the guest hydrophobic molecule during the precipitation step by examining its inclusion properties with genistein. Precipitation of genistein alone resulted in elongated needle-shaped insoluble crystal forms (Fig. 6C), whereas dextran and dextran–genistein precipitation resulted in spherical nanoparticles (Fig. 6B). A comparison of the cryo-TEM images shows that particles that were "closed" in the presence of genistein exhibit a completely different morphology than the dextran or genistein control samples. Dextran particles were of homogeneous density, whereas dextran–genistein particles consisted of a ribbon structure with darker and brighter regions. The darker regions were denser than the brighter ones, and it can be assumed that the dense regions represent the guest molecules of encapsulated genistein. The structure and density dissimilarities suggest dextran–genistein interactions.

Coprecipitation of dextran with genistein by acidification produced three distinct particle-size groups (Table 2): 13% of the particles were in the range of 125–225 nm, 16% were in the range of 740–1000 nm, and 71% were bigger than 2500 nm. The big particles were probably genistein crystals, as seen in the control sample that contained genistein alone (35.5% in the range of 1100–2200 nm and 64.2% bigger than 3000 nm). Thus, coprecipitation by acidification of genistein in the presence of the synthesized dextran increased the percentage of guest molecules in the nanoparticles compared to genistein crystals.

The calculated average surface area-to-volume ratio was higher after the acidification–inclusion procedure containing both dextran and genistein than genistein alone. Even better results were achieved with the DMSO–water coprecipitation. Most of the particles (85%) were in the range of 105–400 nm and only 15% were bigger than 3000 nm, as opposed to genistein alone (99.4% of the particles were bigger than 3000 nm). The average surface area-to-volume ratio of these particles was 10.3 ± 2.2 m^2 mL^{-1}, which is more than threefold that obtained by the acidification method (2.6 ± 0.03 m^2 mL^{-1}). The large insoluble genistein crystals were precipitated out by

centrifugation at 6000 $\times g$ for 20 min, yielding a clear supernatant containing the genistein-loaded dextran nanoparticles. The average surface area-to-volume ratio of these nanoparticles after centrifugation (Table 2) was high (40.3 $\pm$ 10.7 m^2 mL^{-1} and 26.2 $\pm$ 10.5 m^2 mL^{-1} by acidification and DMSO–water methods, respectively).

According to the combined Noyes–Whitney and Nernst equation (eqn (1)), a decrease in particle size increases the specific surface area and, consequently, the dissolution rate and sometimes the solubility:

$$dC/dt = AD(C_s - C)/hV \quad (1)$$

where, dC/dt is the rate of dissolution, A is the surface area presented by the drug/nutraceutical for dissolution, h is the diffusion-layer thickness, D is the diffusion coefficient of the drug/nutraceutical in this layer, C_s is the saturation solubility in the dissolution medium, C is the concentration in the dissolution medium at time t, and V is the volume of the dissolution medium. The reduction in particle size and the increase in solubility will increase the hydrophobic active ingredient's bioavailability, constituting the rationale for using dextran nanoparticles containing the guest nutraceutical.

XRD examination (Fig. 7) of the samples that were washed twice with 50% ethanol exhibited a diffraction pattern similar to that of the synthesized dextran. The decrease in genistein crystallinity can be related to its inclusion in the dextran nanoparticles which prevents the orientation necessary for the flavonoid to crystallize. XRD combined with DLS and cryo-TEM characterization suggested that the crystalline genistein in its native form was altered and an amorphous state was formed. Similar behavior and results have been reported by Motlekar *et al.*,[21] who have investigated genistein-containing poly-(ethylene glycol) microparticles. Data obtained from DSC of the physical mixture of dextran and genistein revealed the disappearance of endothermic genistein peaks for physical mixtures, compared to the pure genistein. This behavior can be related to a decrease in the crystallinity of genistein or to limited changes in its crystalline form. Genistein probably consists of a predominantly amorphous material, since no genistein melting peaks were observed. Based on these observations, Motlekar *et al.*[21] have suggested that the crystalline genistein in its native form was converted to an amorphous form, which explains the absence of a genistein peak in the DSC thermograms. This assumption was verified by melting-point determination, as well as by the higher rates of dissolution because conversion of the genistein into an amorphous form leads to its higher solubility.[21]

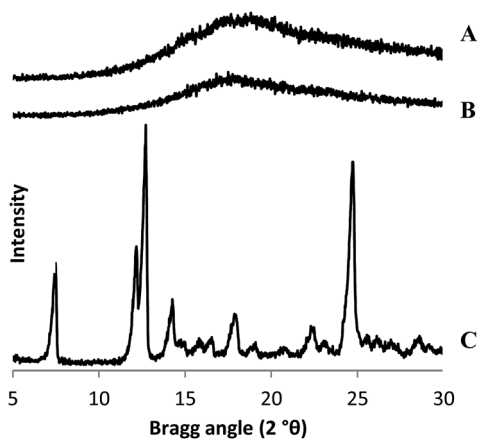

Fig. 7 XRD of (A) synthesized dextran, (B) dextran–genistein after dissolution, coprecipitation, two washes with 50% ethanol and freeze-drying, and (C) genistein.

Thus, genistein inclusion in dextran nanoparticles decreases its particle size, increases its surface area, decreases its crystallinity and consequently increases its solubility, thereby increasing its bioavailability. However, quantification of the genistein content in the washed samples (Table 3) revealed that only small amounts of genistein are loaded into the dextran particles (0.13 $\pm$ 0.07 g genistein per 100 g particles and 0.018 $\pm$ 0.002 g genistein per 100 g particles for acidification and DMSO–water protocols, respectively). We have assumed that the low genistein content was due to the fact that the genistein is only included in the dextran particles, but does not form complexes with the dextran chains as in the case of amylose.[22] After inclusion of genistein in the dextran nanoparticles, the samples were washed to remove the free genistein crystals. The optimal washing solution should be able to dissolve and wash out free genistein crystals without releasing the genistein entrapped in dextran nanoparticles. However, after washing twice with 40–50% ethanol, almost all the genistein was washed away (Fig. 8A). Thus, without strong complexation between genistein and the enzymatically synthesized dextran, most of the entrapped genistein is washed away during the ethanol washing step.

Influence of the lyophilization protocol on inclusion efficiency. The influence of freeze-drying the precipitated genistein-containing dextran nanoparticles before the washing step on their inclusion abilities was examined (Table 3). Dextran–genistein (at a 10 : 1 ratio) nanoparticles were prepared by acidification and DMSO–water protocols. After inclusion of genistein, the samples were freeze-dried. The nanoparticles were washed twice with 40% ethanol and then freeze-dried, and the amount of genistein was quantified. As seen in Table 3, the amount of genistein released by Tris buffer was lower than that released by 80% methanol, suggesting the formation of genistein-containing nanoparticles. Suspension of the nanoparticles in 80% methanol released the total content of the guest molecules, while suspensions in Tris buffer released only the free guest.

Thus, freeze-drying before washing resulted in higher genistein-inclusion efficiency in the nanoparticles produced by both acidification and DMSO–water methods (11- and 141-fold more entrapped genistein, respectively). When the freeze-drying step was carried out before the washing step, inclusion by the DMSO–water method resulted in a higher content of genistein in the nanoparticles compared with the acidification method (5.6 $\pm$ 0.1 and 0.9 $\pm$ 0.05 g genistein per 100 g particles, respectively). Digestion of dextran with dextranase did not release the total genistein content (acidification – 63%;

Table 3 Complexation using an additional freeze-drying step

Inclusion method	Release solution	Extracted genistein (g genistein per 100 g particles)		Genistein entrapped in dextran (g genistein per 100 g particles)
		No freeze-drying	Freeze-drying	
Acidification	80% methanol	0.13 ± 0.07[a]	2.4 ± 0.01	0.9 ± 0.05
	Dextranase	—	1.5 ± 0.02	
	Buffer	0.03 ± 0.001	1.5 ± 0.05	
DMSO–water	80% methanol	0.018 ± 0.002	6.4 ± 0.01	5.6 ± 0.1
	Dextranase	—	1.0 ± 0.1	
	Buffer	0.014 ± 0.002	0.8 ± 0.1	

[a] Standard deviation of means ($n = 2$).

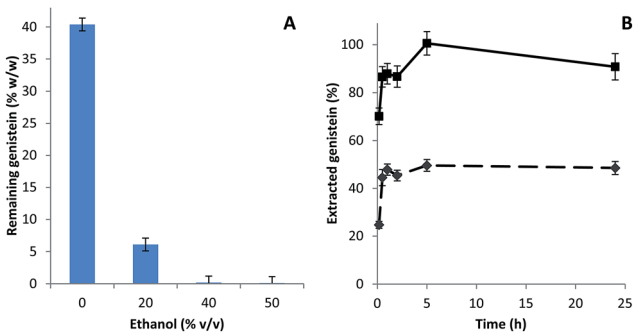

Fig. 8 (A) Dependence of genistein-washing efficiency on ethanol percentage. (B) Dextran–genistein stability after freeze-drying in extrusion solutions: [◆] 50% ethanol–water, and [■] 80% methanol–water (v/v). Error bars represent standard deviation of means ($n = 2$).

DMSO–water – 16%). These findings suggest that the genistein molecules interacted with the dextran and interfered with the dextranase digestion activity.

The influence of freeze-drying on genistein stability in dextran particles was demonstrated by suspending the lyophilized dextran–genistein particles in 50% ethanol overnight (Fig. 8B). The amount of genistein extracted with 50% ethanol was approximately 50% after 0.5 h and it remained at that level for 24 h; during the same time period, almost total genistein extraction occurred with the non-freeze-dried sample in 50% ethanol (Fig. 8A). These results can be attributed to the presence of strong interactions between the dextran and genistein after freezing and mainly during the drying stage, which are not weakened by the addition of 50% ethanol. The increased genistein-inclusion efficiency following the additional lyophilization step can be related to the formation of hydrogen bonds and to the occurrence of van der Waals interactions between the dextran and the hydrophobic guest molecule. During the drying stage of lyophilization, water molecules are removed from the entrapped genistein nanoparticles by sublimation and diffusion. This dehydration process probably leads to the formation of new hydrogen bonds between C═O, –O–, and the three –OH groups of genistein and hydroxyl groups of the polysaccharide dextran, in addition to the enhanced van der Waals interactions. Cohen[35] suggested that hydrogen bonds may also be involved in the inclusion/complexation of genistein with amylose helices, and that the complexation process creates new hydrogen bonds. Thus, one plausible explanation is that dehydration initiates the formation of those hydrogen bonds.

Another explanation might be based on the interaction between the hydrophobic guest molecules, trapped inside or between the coils created by the dextran chains. In this case, the dextran–genistein interaction would interfere with the dextranase digestion activity, leading to a partial genistein release, and initiating a negative correlation between the quantity of entrapped genistein and the percentage released by the dextranase digestion activity.

The samples prepared by the DMSO–water protocol had a higher content of entrapped genistein and a respectively smaller release percentage by dextransucrase in comparison with the acidification method. Thus, the DMSO–water protocol is more suitable for inclusion/complexation of genistein. In addition, enzymatically synthesized dextran nanoparticles offer some advantages over amylose, HACS (high amylose corn starch), PEG and Eudragit (Table 4). Cohen *et al.* 2008 (ref. 22) have prepared complexes of amylose and of high-amylose corn starch (HACS) with genistein by applying the acidification method. The amylose-genistein and HACS–genistein complexes exhibited higher genistein content (11.3 ± 1.7 g genistein per 100 g particles and 9.3 ± 1.5 g genistein per 100 g particles, respectively) compared to inclusion in dextran nanoparticles (5.6 ± 0.1 g genistein per 100 g particles) in this study. However, the main advantage of genistein inclusion in enzymatically synthesized dextran lies behind the production of genistein loaded nano particles (85% of the particles were in range of 105–400 nm), compared to amylose 93 ± 36 μm or HACS 23 ± 11

Table 4 Genistein inclusion in enzymatically synthesized dextran compared to other carriers

Carrier	Optimal loading [g 100 g^{-1}]	Particle size
Dextran	5.6 ± 0.1	105–400 nm
Amylose[22]	11.3 ± 1.7	93 ± 36 μm
HACS[22]	9.3 ± 1.5	23 ± 11 μm
PEG[21]	5.92 ± 0.21	10–50 μm
Eudragit E100[20]	5.02 ± 0.04	120.0 ± 9.25 nm

μm microparticles. PEG microparticles containing genistein were produced by Motlekar *et al.* (ref. 21) by solvent evaporation using an alcohol-in-oil protocol. The optimal loading of the genistein micro-particles was 5.92 ± 0.21 g genistein per 100 g particles. The size of the genistein particles was in range of 10–50 μm. In contrast to PEG, the main advantage of genistein inclusion in enzymatically synthesized dextran was production of genistein loaded nano particles in a food-grade matrix. Tang *et al.* 2011 (ref. 20) have obtained results similar to our present work, investigating genistein nano-encapsulation in Eudragit E100. Genistein nanoparticles prepared by the nano-precipitation technique showed a blue opalescent and uniform appearance. The optimal drug loading of the genistein nanoparticle formulation was 5.02 ± 0.04 g genistein per 100 g particles. The size of the genistein nanoparticles was approximately 120.0 ± 9.25 nm when diluted 100 times with distilled water.[20] However, additional advantage over using PEG or Eudragit E100 actually lies in the use of pure dextran as the material for the entire nanocapsule production by turning dextran into a potential carrier system in the field of hydrophobic nutraceuticles such as the isoflavone.

Conclusions

The overall goal of this study was to develop nanosized vehicles, based on new polysaccharide architectures produced by enzymatic synthesis that could entrap hydrophobic nutraceuticals of low water solubility. To achieve this objective, we have developed the dextransucrase synthesis procedure to produce nanosized vehicles for the hydrophobic nutraceutical genistein. The influence of various conditions on dextran synthesis was investigated with the aim of optimizing the synthesis of pure dextran as the material for the entire nanoparticle instead of only its coating or to make a copolymer. It was concluded that the dextran polymerization rate and the product volume/size distribution depend strongly on the pH of the reaction buffer. At low enzyme concentrations, the dextran chains were longer; thus, to produce smaller dextran particles (≤100 nm), the optimal conditions were: pH 5.2–6 and ≤0.5 M sucrose. Higher pH resulted in slower synthesis rate, partial substrate utilization and bigger dextran particles. In the second stage, we have evaluated inclusion/complexation capabilities of enzymatically synthesized dextran nanoparticles. Two inclusion methods were employed: DMSO–water and acidification. Optimization of the inclusion processes led to the production of nanosized dextran particles containing genistein. The DMSO–water inclusion protocol has been found to be more suitable for the inclusion of genistein in the enzymatically synthesized dextran, resulting in a higher content (5.6 ± 0.1 g genistein per 100 g particles), a higher percentage of nanosized particles (85%, 105–400 nm; $A/V_p = 26.2 \pm 10.5$ m^2 mL^{-1}), and an increase in the average A/V_p more than threefold compared with the acidification protocol. For both inclusion protocols—acidification and DMSO–water—freeze-drying prior to the washing step increased the yield of the included nutraceutical (by 11- and 141-fold, respectively) presumably due to the formation of new hydrogen bonds and van der Waals interactions during the drying stage. These interactions led to the formation of complexes between the hydrophobic inner part of the dextran and the genistein.

Materials and methods

Materials

Dextransucrase from *Leuconostoc mesenteroides* D9909 was from Sigma-Aldrich Chemicals Co. (St. Louis, MO). Dextranase [1,6-α-D-glucan 6-glucanohydrolase] from *Penicillium* sp. (crude, Sigma-Aldrich) was used for enzymatic digestion of the dextran. Sucrose was from Sigma-Aldrich, and genistein from LC Labs (Woburn, MA, BNG-6055). Potassium hydroxide (KOH), hydrogen chloride (HCl), calcium chloride ($CaCl_2$), dimethylsulfoxide (DMSO), methanol, ethanol and all other reagents were analytical-grade chemicals.

Dextran synthesis by the enzyme dextransucrase

Dextransucrases synthesize dextran from sucrose. *Leuconostoc* and *Streptococcus* are the main bacterial genera recognized to produce these enzymes.[31] Dextran is a glucan with α-(1 → 6) linked glucose in the main chain,[31] and its structure differs in length depending on the enzyme's bacterial source. The main branching linkage is α-(1 → 3), but α-(1 → 2) and α-(1 → 4) linkages are also known.[31] The reaction of dextransucrases leads to the synthesis of dextran from sucrose:

$$n\text{sucrose} \rightarrow (\text{glucose})_{n-m-w} + n - m\text{fructose} + m\text{leucrose} + w\text{glucose}.$$

This reaction is essentially irreversible[31] and the main products are high-molecular-weight dextran [1×10^7 to 1×10^8 Da] and fructose. Glucose arises from an acceptor reaction with water, and leucrose from an acceptor reaction with fructose.[31] Dextransucrases use the α-(1 → 2) glycosidic bond in the sucrose molecule as an energy source for polysaccharide and oligosaccharide synthesis.[31] Branching of the dextran chain is catalyzed by dextransucrase itself.[36] The dextran chain serves as an acceptor molecule in which a 3-hydroxyl group of an internal glucose generates nucleophilic attack at the C_1 of either the glucosyl–enzyme complex or the dextranyl-enzyme complex. In this process, an α-(1 → 3) branching linkage is formed between the dextran acceptor chain and a glucosyl moiety or the dextranyl chain.

Enzymatic synthesis protocol. The enzymatic synthesis was carried out at room temperature (25 °C) in 20 mM sodium acetate buffer, pH 5.2 with 1 mM $CaCl_2$. Reactions at higher pH were carried out in phosphate buffers. The reaction involved dextransucrase and sucrose. Samples were taken at various time intervals, and the reaction was terminated by heating the sample at 65 °C for 10 min. Dextransucrase activity was determined by following the release of fructose and glucose and the formation of dextran. The release of fructose and glucose was measured by high-performance anion-exchange chromatography using pulsed amperometric detection (HPAEC-PAD) (Dionex LC30 instrument (Sunnyvale, CA) equipped with a pulsed amperometric detector (ED40) and a PA1 column). Isocratic elution was performed with 150 mM NaOH as the mobile

phase at a flow rate of 1 mL min^{-1}. Sucrose conversion by dextransucrase yields glucose, which can be incorporated into the growing polymer (formation of dextran) and fructose in a 1 : 1 ratio to the amount of sucrose converted. The amount of fructose reflects the total amount of sucrose utilized during the reaction (total activity). The amount of free glucose is a measure of hydrolytic activity of the enzyme. Thus, subtracting the amount of glucose from fructose provides the polymerization activity.[26]

Synthesis of polysaccharide particles in aqueous solution elevates the turbidity of the suspension, and the turbidity increase is therefore a simple and useful parameter for controlling the polymerization reaction: optical density at 600 nm is measured (Ultrospec™ 2100 pro, Amersham Pharmacia Biotech, NJ) at 10 min intervals. In addition, the final turbidity of the samples, after mixing, was determined. The effects of several reaction parameters on the synthesis—reaction pH (5.2–8 at a constant dextransucrase concentration of 0.42 U mL^{-1} and sucrose concentration of 50 mM), enzyme concentration (0.1 and 0.42 U mL^{-1} at a constant sucrose concentration of 50 mM), and sucrose concentration (0.002–3 M at a constant dextransucrase concentration of 0.42 U mL^{-1})—were determined.

Dextran purification. To purify the synthesized dextran, salts and short oligosaccharides need to be removed from the enzymatic mixture. The purification was carried out in the following steps: (1) dextran was precipitated by adding ethanol to the enzymatic reaction mixture to a final concentration of 50% (v/v). The samples were then vortexed and placed on ice. Phase separation was carried out by centrifugation (10 000 $\times g$, 15 min) and the supernatant was discarded; (2) the wet pellet was washed twice with an ethanol–water mixture (50/50 v/v) and centrifuged as before. The supernatant was discarded; (3) the pellet was lyophilized. After the purification process the synthesized dextran was weighed and the dextran yield was calculated as follows:

$$\text{Dextran yield } (\%) = \frac{\text{lyophilized dextran (mg)}}{\text{theoretical dextran amount (mg)}} \times 100 \quad (2)$$

where the theoretical dextran amount (mg) was calculated as total utilization of glucose out of sucrose.

Lyophilization method. Samples were frozen in −80 °C freezers until thermal equilibrium (120 min). After freezing, samples were freeze-dried using a SECFROID RIN-1362 lyophilizer (Lausanne, Switzerland) at a constant controlled shelf temperature of −14 °C and 0.1 mbar for 48 h.

Inclusion/complexation protocols

The freeze-dried dextran powder was tested for complexation ability by applying two protocols: (1) inclusion/complexation *via* dilution of DMSO in water; (2) inclusion/complexation *via* decreasing pH.

DMSO in water method. Inclusion/complexation of genistein to the synthesized dextran *via* dilution of a DMSO mixture was based on a previously described method[23,37] for creating V-amylose complexes.[38] This process is based on coprecipitation of the synthesized polysaccharide and the guest molecule from an aqueous solution. Both components are first solubilized in DMSO, which dissolves both polar and nonpolar compounds, and then the mixture is diluted with water, leading to coprecipitation of polysaccharide–guest complexes. The rationale for this protocol is the solubility of polysaccharides and hydrophobic guest molecules in DMSO. When this mixture is diluted 20-fold with water, the hydrophobic guest molecules become insoluble, thereby enhancing polysaccharide–guest interactions as well as interhelical interactions of the polysaccharides. To apply this protocol to enzymatically synthesized dextran nanoparticles, 0.1 mL DMSO preheated to 90 °C was used to gradually dissolve the dextran and genistein. The resulting clear DMSO solution was rapidly added to 1.9 mL distilled water (preheated to 90 °C) with vigorous stirring, incubated for 15 min at 90 °C, and then separated after cooling the suspension on ice for 30 min. All samples were then centrifuged (20 000 $\times g$, 25 min, 4 °C), the supernatant was discarded, and the precipitate was washed twice with an ethanol–water mixture (0–50% v/v ethanol) and centrifuged. The complexes were then freeze-dried for further examination.

Acidification method. This inclusion/complexation process is based on coprecipitation of the polysaccharide and the guest molecule from an aqueous solution. Both components are first solubilized at an alkaline pH. Inclusion/complexation is then carried out by acidifying the solution (KOH/H_3PO_4) as previously described for other compounds,[22,23,39] and the polysaccharide–guest complexes precipitate out. Ionization of the polysaccharide's hydroxyl groups enhances their solubility in aqueous solutions due to electrostatic repulsion, and therefore the rationale for this protocol is based on deprotonation of hydroxyl groups of the polysaccharides and guest molecules at high pH. The ionization of matrix components at high pH enhances their solubility in water, leading to molecular solubilization of both polysaccharides and guest molecules. When the pH is lowered below the pK_a of the hydroxyl groups, the protonated form of these groups renders the complexing molecules less soluble in water, thereby enhancing the dextran–genistein interactions.

The synthesized dextran was dissolved in 0.1 N KOH solution (6 mL, 10 mg mL^{-1} of 0.1 N KOH, pH 12.5) at 90 °C. A guest-compound solution was prepared separately at 30 °C (4 mL, 1.5 mg mL^{-1} of 0.1 N KOH, pH 12.5). The solutions were mixed at 30 °C, and the mixture was precipitated by adjusting the pH to 4.7 (±0.5) with 2% H_3PO_4, and holding it for 24 h under gentle stirring. All samples were then centrifuged (20 000 $\times g$, 25 min, 4 °C), the supernatant was discarded, and the precipitate was washed twice with an ethanol–water mixture (0–50% ethanol) and centrifuged. The complexes were then freeze-dried for further examination.

Optimization of the washing step

To remove free genistein molecules without releasing the genistein entrapped in the dextran nanoparticles, the effect of percent ethanol in the washing mixture was investigated. Complexes prepared *via* the DMSO–water method were washed

twice with different ethanol–water mixtures (0, 20, 40 and 50% ethanol). After each rinse step, the samples were centrifuged (20 000 $\times g$, 25 min, 4 °C) and the supernatant was discarded. The content of the remaining genistein was then determined.

Determination of genistein content

After inclusion in the synthesized dextran (0.1 U mL^{-1} dextransucrase and 150 mM sucrose), genistein content in the nanoparticle complex was determined by HPLC using previously described protocols.[22] The guest molecule was extracted with 80% methanol: the nanoparticle complex (15 mg) was incubated with 1 mL 80% methanol at 30 °C overnight. The content of free genistein was determined by incubating the complex in Tris buffer at 30 °C overnight. Since genistein is poorly soluble in water, after the incubation, samples were diluted with the buffer to a concentration below their solubility limit.[40] The solution was then centrifuged (5 500 $\times g$, 15 min). Genistein was quantified from the supernatant by reverse-phase (RP) HPLC, using an HP 1100 equipped with a diode array detector and an autosampler and controlled by ChemStation software (Hewlett-Packed, Wilmington, DE). HPLC analysis was carried out on a reverse-phase C_{18} column (250 × 4 mm with 5 μm packing). Samples were eluted at a flow rate of 1 mL min^{-1} with solvent A (0.1% acetic acid in water, v/v) and solvent B (acetonitrile). The gradient elution was from 5 to 35% solvent B in a linear gradient over 33 min, washing with 100% solvent B for 5 min, and then equilibrating for 10 min between runs with 5% solvent B. The injection volume was 20 μL, and detection was performed by UV absorbance at 254 nm.[41] The amount of genistein in the inclusion complex was determined with the help of a calibration curve using pure genistein as the standard.

The released genistein (mg) was used to calculate genistein inclusion/complexation efficiency (% w/w) and genistein loading (% w/w). Genistein inclusion efficiency was calculated as follows:

$$\text{Inclusion efficiency } (\%) = \frac{\text{encapsulated guest (mg)}}{\text{initial guest mass (mg)}} \quad (3)$$

where initial guest mass (mg) is the amount of genistein added to the inclusion/complexation mixture, and encapsulated guest (mg) is the amount of genistein recovered from the nanoparticles.

Genistein loading in the complex was calculated per 100 mg complex using the following equation:

$$\text{Guest loading } (\%) = \frac{\text{mass of guest in the nanoparticles (mg)}}{\text{mass of nanoparticles recovered (mg)}} \times 100 \quad (4)$$

The amount of genistein entrapped in dextran (g genistein per 100 g particles) was calculated using the following equation:

$$\text{Entrapped guest in the particles } (\%) = \text{guest loading } (\%) - \text{free guest } (\%) \quad (5)$$

where guest loading is the content of genistein extracted with 80% methanol and free guest is the content of genistein extracted with buffer.

Enzymatic digestion

The purpose of this test was to quantify the amount of guest released from the dextran nanoparticles by enzymatic digestion. A mixture of the complexes and dextranase in Tris buffer (12.9 U mL^{-1} enzyme, 10 mM Tris, pH 6.7) was held at 37 °C overnight under gentle stirring.[42] The amount of genistein released from the complex was calculated based on the total genistein content in the complex. The amount of genistein released was compared to the amount that was released in the buffer solution without dextranase (24 h at 37 °C).

Characterization of the dextran and genistein-complexated particles

Particles and their complexes were characterized by dynamic light scattering (DLS), cryogenic-transmission electron microscopy (cryo-TEM) and X-ray diffraction (XRD).

DLS. Particle size distribution was studied by using a dynamic light scattering (DLS) analyzer (NICOMP™ 380, Particle Sizing Systems Inc., Santa Barbara, CA, USA) equipped with an Avalanche Photo Diode (APD) detector, used at a fixed angle of 90°. The 90 mW laser wavelength was 658 nm. All the samples were diluted with water in order to avoid errors due to interparticle interactions and/or multiple scattering, therefore the viscosity of the medium was set to 0.933 cp. A 500 μL aliquot of the suspended sample was inserted into 6 × 50 mm borosilicate glass tubes. The data were recorded over a period of 10 min. Measurements were made in duplicate at 25 °C. Gaussian mono-modal distribution analysis and Nicomp mono-bi- or tri-modal distributions were calculated from the scattered light intensity fluctuations, by cumulants Nicomp™ analysis of the auto correlation function (see ESI in ref. 43 for a more complete method description). The volume-weighted particle size distribution was calculated assuming that the particle were spheres of uniform density (software default). To compare different samples, the percent distribution intensity was calculated as follows:

$$\text{Distribution } (D_i) = \frac{\text{volume intensity } (D_i)}{\text{total intensity}} \times 100\% \quad (6)$$

Based on the assumption that all the particles were spherical, the average surface area-to-volume ratio was calculated using eqn (7), in which A is the particle surface area, V_p the particle volume, and D_p its diameter.

$$A/V_p = (\pi D_p^2)/(\pi D_p^3/6) = 6/D_p \quad (7)$$

Cryo-TEM. Cryo-TEM was used to determine the detailed morphology of the enzymatically synthesized product or inclusion complexes. Samples were prepared in a Vitrobot (FEI), an automated specimen-preparation device. The solution was

equilibrated in the Vitrobot at 25 °C for 20 min, at full water saturation, to avoid evaporation of volatile components from the sample during specimen preparation. Specimens were prepared on a 400-mesh copper grid coated with a perforated film, held by tweezers in the Vitrobot. A small drop (5 to 8 μL) was applied to the grid and blotted with a filter paper for 1 s to form a thin liquid film. The blotted sample was immediately plunged into liquid ethane at its freezing point to produce a vitrified sample, and then transferred to liquid nitrogen for storage. Samples were examined using a Philips Tecnai 12 G2 TEM, at 120 kV with a Gatan cryo-holder maintained below −173 °C. Images were recorded on an Ultrascan 1000 2k × 2k CCD camera using the Digital Micrograph software package, under low-dose conditions to minimize the electron-beam-radiation damage. Brightness and contrast were enhanced using the Adobe Photoshop 7.0ME package.

XRD. To verify the formation of a new structure after complexation by the acidification method, *i.e.* a structure that differs from those of genistein and synthesized dextran, complexes were analyzed by XRD. XRD measurements were carried out using a Philips PW 3020 powder diffractometer equipped with a graphite crystal monochromator. The operating conditions were: CuKα1 radiation (0.154 nm), 40 kV and 40 mA current. Samples were scanned over the range of 5–35 °2θ in steps of 0.02 °2θ per 4 s, and the crystalline nature of the complex was determined by the position of the peaks.

Data and statistical analyses

All experiments were performed with at least three repetitions, and results are expressed as mean ± standard deviation (SD). Where relevant, the number of repetitions is specified in the text. The significance of the differences between groups was tested by *t*-test. A probability level (P) of < 0.05 was considered to be statistically significant unless otherwise specified. Statistical analysis was performed using the data analysis tool pack of Microsoft Excel 2007.

Acknowledgements

This work was supported by the Niedersachsen – Israel Research Cooperation Program, the State of Lower Saxony and the Volkswagen Foundation, Hannover, Germany. We thank the Russell Berrie Nanotechnology Institute and the Lorry I. Lokey Interdisciplinary Center for Life Science and Engineering, Technion for partial support. Y.S. holds the Erwin and Rosl Pollak Chair in Biotechnology at the Technion.

References

1 L. Sagalowicz and M. E. Leser, *Curr. Opin. Colloid Interface Sci.*, 2010, **15**, 61–72.
2 R. C. Benshitrit, C. S. Levi, S. L. Tal, E. Shimoni and U. Lesmes, *Food Funct.*, 2012, **3**, 10–21.
3 U. Lesmes and D. J. McClements, *Trends Food Sci. Technol.*, 2009, **20**, 448–457.
4 D. J. McClements and Y. Li, *Adv. Colloid Interface Sci.*, 2010, **159**, 213–228.
5 Y. Shoji and H. Nakashima, *J. Drug Targeting*, 2004, **12**, 385–391.
6 K. P. Velikov and E. Pelan, *Soft Matter*, 2008, **4**, 1964–1980.
7 Y. Avior, D. Bomze, O. Ramon and Y. Nahmias, *Food Funct.*, 2013, **4**, 831–844.
8 A. Crozier, I. B. Jaganath and M. N. Clifford, *Nat. Prod. Rep.*, 2009, **26**, 1001–1043.
9 M. Kano, T. Takayanagi, K. Harada, S. Sawada and F. Ishikawa, *J. Nutr.*, 2006, **136**, 2291–2296.
10 S. Banerjee, Y. W. Li, Z. W. Wang and F. H. Sarkar, *Cancer Lett.*, 2008, **269**, 226–242.
11 H. Adlercreutz, H. Markkanen and S. Watanabe, *Lancet*, 1993, **342**, 1209–1210.
12 R. A. Dixon and D. Ferreira, *Phytochem. Rev.*, 2002, **60**, 205–211.
13 L. Jian, *Mol. Nutr. Food Res.*, 2009, **53**, 217–226.
14 Y. Ungar, O. F. Osundahunsi and E. Shimoni, *J. Agric. Food Chem.*, 2003, **51**, 4394–4399.
15 A. Rubinstein, *Drug Discovery Today: Technol.*, 2005, **2**, 33–37.
16 W. Helbert and H. Chanzy, *Int. J. Biol. Macromol.*, 1994, **16**, 207–213.
17 E. Acosta, *Curr. Opin. Colloid Interface Sci.*, 2009, **14**, 3–15.
18 V. Maravajhala, S. Papishetty and S. Bandlapalli, *Int. J. Pharma Sci. Res.*, 2012, **3**, 84–96.
19 C. F. Chau, S. H. Wu and G. C. Yen, *Trends Food Sci. Technol.*, 2007, **18**, 269–280.
20 J. Tang, N. Xu, H. Ji, H. Liu, Z. Wang and L. Wu, *Int. J. Nanomed.*, 2011, **6**, 2429.
21 N. Motlekar, M. A. Khan and B. B. C. Youan, *J. Appl. Polym. Sci.*, 2006, **101**, 2070–2078.
22 R. Cohen, Y. Orlova, M. Kovalev, Y. Ungar and E. Shimoni, *J. Agric. Food Chem.*, 2008, **56**, 4212–4218.
23 I. Lalush, H. Bar, I. Zakaria, S. Eichler and E. Shimoni, *Biomacromolecules*, 2005, **6**, 121–130.
24 R. Stancanelli, A. Mazzaglia, S. Tommasini, M. Calabrò, V. Villari, M. Guardo, P. Ficarra and R. Ficarra, *J. Pharm. Biomed. Anal.*, 2007, **44**, 980–984.
25 V. R. Sinha and R. Kumria, *Int. J. Pharm.*, 2001, **224**, 19–38.
26 D. Goldman, N. Lavid, A. Schwartz, G. Shoham, D. Danino and Y. Shoham, *J. Biol. Chem.*, 2008, **283**, 32209–32217.
27 D. Kim, J. F. Robyt, S. Y. Lee, J. H. Lee and Y. M. Kim, *Carbohydr. Res.*, 2003, **338**, 1183–1189.
28 A. K. Goulas, *Enzyme Microb. Technol.*, 2004, 327–338.
29 K. Heincke, B. Demuth, H.-J. Jördening and K. Buchholz, *Enzyme Microb. Technol.*, 1999, **24**, 523–534.
30 P. Monsan, *Zuckerindustrie*, 1995, **120**, 705–707.
31 J. F. Robyt, *Adv. Carbohydr. Chem. Biochem.*, 1995, **51**, 133–168.
32 A. Tanriseven and J. F. Robyt, *Carbohydr. Res.*, 1993, **245**, 97–104.
33 M. J. Habib, *Pharmaceutical solid dispersion technology*, CRC Press, 2001.
34 S. Sethia and E. Squillante III, *Crit. Rev. Ther. Drug. Carrier. Syst.*, 2003, **20**, 34.
35 R. Cohen, B. Schwartz, I. Peri and E. Shimoni, *J. Agric. Food Chem.*, 2011, **59**, 7932–7938.

36 J. F. Robyt and H. Taniguchi, *Arch. Biochem. Biophys.*, 1976, **174**, 129–135.
37 J. Karkalas, S. Ma, W. R. Morrison and R. A. Pethrick, *Carbohydr. Res.*, 1995, **268**, 233–247.
38 U. Lesmes, S. H. Cohen, Y. Shener and E. Shimoni, *Food Hydrocolloids*, 2009, **23**, 667–675.
39 B. Conde-Petit, F. Escher and J. Nuessli, *Trends Food Sci. Technol.*, 2006, **17**, 227–235.
40 D. Li, S.-A. Roh, J.-H. Shim, B. Mikami, M.-Y. Baik, C.-S. Park and K.-H. Park, *J. Agric. Food Chem.*, 2005, **53**, 6516–6524.
41 A. P. Griffith and M. W. Collison, *J. Chromatogr. Sep. Tech.*, 2001, **913**, 397–413.
42 S. Ahmad, R. F. Tester, A. Corbett and J. Karkalas, *Carbohydr. Res.*, 2006, **341**, 2694–2701.
43 A. Shapira, Y. G. Assaraf and Y. D. Livney, *Nanomedicine: Nanotechnology, Biology and Medicine*, 2010, **6**, 119–126.